REPORT DOCUMENTATION PAGE

Form Approved OMB NO. 0704-0188

1. REPORT DATE (DD-MM-YYYY)	2. REPORT TYPE	3. DATES COVERED (From - To)
31-08-2012	Conference Proceeding	-

4. TITLE AND SUBTITLE
Synthetic aperture acoustic imaging of non-metallic cords

5a. CONTRACT NUMBER
W911NF-09-1-0082

5b. GRANT NUMBER

5c. PROGRAM ELEMENT NUMBER
633606

6. AUTHORS
Aldo A. J. Glean, Chelsea E. Good, Joseph F. Vignola, John A. Judge, Teresa J. Ryan, Steven S. Bishop, Peter M. Gugino, Mehrdad Soumekh

5d. PROJECT NUMBER

5e. TASK NUMBER

5f. WORK UNIT NUMBER

7. PERFORMING ORGANIZATION NAMES AND ADDRESSES
The Catholic University of America
The Catholic University of America
620 Michigan Avenue, N.E.
Washington, DC 20064 -

8. PERFORMING ORGANIZATION REPORT NUMBER

9. SPONSORING/MONITORING AGENCY NAME(S) AND ADDRESS(ES)
U.S. Army Research Office
P.O. Box 12211
Research Triangle Park, NC 27709-2211

10. SPONSOR/MONITOR'S ACRONYM(S)
ARO

11. SPONSOR/MONITOR'S REPORT NUMBER(S)
55997-CS.3

12. DISTRIBUTION AVAILIBILITY STATEMENT
Approved for public release; distribution is unlimited.

13. SUPPLEMENTARY NOTES
The views, opinions and/or findings contained in this report are those of the author(s) and should not contrued as an official Department of the Army position, policy or decision, unless so designated by other documentation.

14. ABSTRACT
This work presents a set of measurements collected with a research prototype synthetic aperture acoustic (SAA) imaging system. SAA imaging is an emerging technique that can serve as an inexpensive alternative or logical complement to synthetic aperture radar (SAR). The SAA imaging system uses an acoustic transceiver (speaker and microphone) to project acoustic radiation and record backscatter from a scene. The backscattered acoustic energy is used to generate information about the location, morphology, and mechanical properties of various objects. SAA

15. SUBJECT TERMS
Synthetic aperture acoustic, acoustic imaging, image reconstruction

16. SECURITY CLASSIFICATION OF:			17. LIMITATION OF ABSTRACT	15. NUMBER OF PAGES	19a. NAME OF RESPONSIBLE PERSON
a. REPORT	b. ABSTRACT	c. THIS PAGE			Joseph Vignola
UU	UU	UU	UU		19b. TELEPHONE NUMBER: 202-319-6132

Report Title

Synthetic aperture acoustic imaging of non-metallic cords

ABSTRACT

This work presents a set of measurements collected with a research prototype synthetic aperture acoustic (SAA) imaging system. SAA imaging is an emerging technique that can serve as an inexpensive alternative or logical complement to synthetic aperture radar (SAR). The SAA imaging system uses an acoustic transceiver (speaker and microphone) to project acoustic radiation and record backscatter from a scene. The backscattered acoustic energy is used to generate information about the location, morphology, and mechanical properties of various objects. SAA detection has a potential advantage when compared to SAR in that non-metallic objects are not readily detectable with SAR. To demonstrate basic capability of the approach with non-metallic objects, targets are placed in a simple, featureless scene. Nylon cords of five diameters, ranging from 2 to 15 mm, and a joined pair of 3 mm fiber optic cables are placed in various configurations on flat asphalt that is free of clutter. The measurements were made using a chirp with a bandwidth of 2-15 kHz. The recorded signal is reconstructed to form a two-dimensional image of the distribution of acoustic scatterers within the scene. The goal of this study was to identify basic detectability characteristics for a range of sizes and configurations of non-metallic cord. It is shown that for sufficiently small angles relative to the transceiver path, the SAA approach creates adequate backscatter for detectability.

Conference Name: SPIE Defence Sensing

Conference Date: April 23, 2012

Synthetic aperture acoustic imaging of non-metallic cords

Aldo A. J. Glean, Chelsea E. Good, Joseph F. Vignola*, John A. Judge, Teresa J. Ryan
Center for Acoustics, Vibration, and Structures
Department of Mechanical Engineering
The Catholic University of America, 620 Michigan Ave, NE
Washington, DC 20064

Steven S. Bishop, Peter M. Gugino
US Army RDECOM CERDEC NVESD
10221 Burbeck Rd., Ft. Belvoir, VA 22060

Mehrdad Soumekh
Soumekh Consulting, Bethesda, MD, 20817

ABSTRACT

This work presents a set of measurements collected with a research prototype synthetic aperture acoustic (SAA) imaging system. SAA imaging is an emerging technique that can serve as an inexpensive alternative or logical complement to synthetic aperture radar (SAR). The SAA imaging system uses an acoustic transceiver (speaker and microphone) to project acoustic radiation and record backscatter from a scene. The backscattered acoustic energy is used to generate information about the location, morphology, and mechanical properties of various objects. SAA detection has a potential advantage when compared to SAR in that non-metallic objects are not readily detectable with SAR. To demonstrate basic capability of the approach with non-metallic objects, targets are placed in a simple, featureless scene. Nylon cords of five diameters, ranging from 2 to 15 mm, and a joined pair of 3 mm fiber optic cables are placed in various configurations on flat asphalt that is free of clutter. The measurements were made using a chirp with a bandwidth of 2-15 kHz. The recorded signal is reconstructed to form a two-dimensional image of the distribution of acoustic scatterers within the scene. The goal of this study was to identify basic detectability characteristics for a range of sizes and configurations of non-metallic cord. It is shown that for sufficiently small angles relative to the transceiver path, the SAA approach creates adequate backscatter for detectability.

Keywords: Synthetic aperture acoustic, acoustic imaging, image reconstruction

1. INTRODUCTION

In recent years, the interest in technology for imaging of roadsides and roadbeds has intensified. These technologies find application in the protection of convoys from concealed threats. Side-scanning synthetic aperture imaging can be used in this way to monitor the roadsides. This imaging approach uses a co-located source and receiver to broadcast and collect signals perpendicular to the instrument's travel direction. Side-scanning synthetic aperture imaging systems can use either electromagnetic or acoustic radiation[1] of varying wavelengths to illuminate targets. Various bands of the electromagnetic spectrum can be used, such as radar[2] or, less commonly, visible light or infrared. The use of acoustic radiation as an alternative to electromagnetic provides a few advantages. A system that uses acoustic radiation, like the SAA (Synthetic Aperture Acoustic) system described in this work, is less expensive to build than its electromagnetic source counterpart, human exposure concerns are lower, and the presence of metal or moisture in a target scene does not obscure the image. In this paper, measurements were made within the audio frequency range (2 -15 kHz) which

* vignola@cua.edu; phone 202-319-6132; fax 202-319-5173

corresponds to wavelengths of 2.3 -17.1 cm. This range overlaps with that used for typical ground-penetrating SAR (synthetic aperture radar), which has wavelengths of 12.5-37.5 cm at a frequency range of 0.8-2.4 GHz.

As mentioned, this SAA[3] system simultaneously broadcasts and collects an acoustic signal using a single source and receiver, thereby creating a synthetic array of sensors by the motion of the transceiver. The aperture size of the synthetic array is relatively large due to the typically long travel distance, which also translates into good spatial resolution[4]. This detection approach relies on the backscatter from the targets and the surrounding scene. Material properties (stiffness, density, and absorption), geometry (size and shape), and physical layout of the scene can affect the backscatter in important ways that allow for discrimination of specific objects in the reconstructed image. The strengths and capabilities of the SAA technique makes it well-suited as a complement to SAR.

This paper summarizes a set of experiments that focus on the observability of nonmetallic cords. The intention is to present an extremely simple case to highlight the basic capability of the approach. A simple scene (nominally flat asphalt surface with no clutter objects) is used to study a set of nylon cords with diameters ranging from approximately 3 to 16 mm at a set of angles from parallel to the transceiver path up to 30 degrees. This study indicates that for a range of angles, the SAA technique is capable of nylon cord detection and the detection is sensitive to, amongst other factors, include the angle with respect to the transceiver path.

2. SYNTHETIC APERTURE SYSTEM

The experimental equipment used for this study is shown in Fig. 1. The transceiver uses a Pyramid TW67 Tweeter as a source and a B&K 4265 ½ inch microphone to record the backscattered acoustic signal. The microphone is placed within a conical funnel to increase its directionality, and is mounted directly above the speaker. The speaker/microphone assembly is mounted on a tripod with adjustable height, azimuth, and squint angle. A camera is also attached to the side of the transceiver assembly. Photographs of the scene are recorded at regular intervals during data collection to serve as a reference to objects in the reconstructed image. Both wheels of the trailer are instrumented with rotary encoders to allow determination of the transceiver location and travel trajectory at each instant. The trailer also carries the data acquisition system, which consists of a Intel based computer running the Microsoft Windows operating system with a National Instruments data acquisition card and LabVIEW® software, a patch box for connecting external equipment to the data acquisition card, analog filter for out-of-band noise suppression, and an audio power amplifier for the loudspeaker signal. A portable gasoline-powered generator provides electrical power to all components. Future versions of this system could integrate many of these components into the towing vehicle itself. During operation, the experiment is controlled from the cab of the tow vehicle using an Ethernet connection from an operator's laptop. A schematic of the system, showing signal paths and various system components, is shown in Fig. 1. The loudspeaker signal is a linear FM chirp of 2-17 kHz to which a power window[5] (sometimes also referred to as an exponential window) has been applied to limit spectral leakage (see Fig. 2).

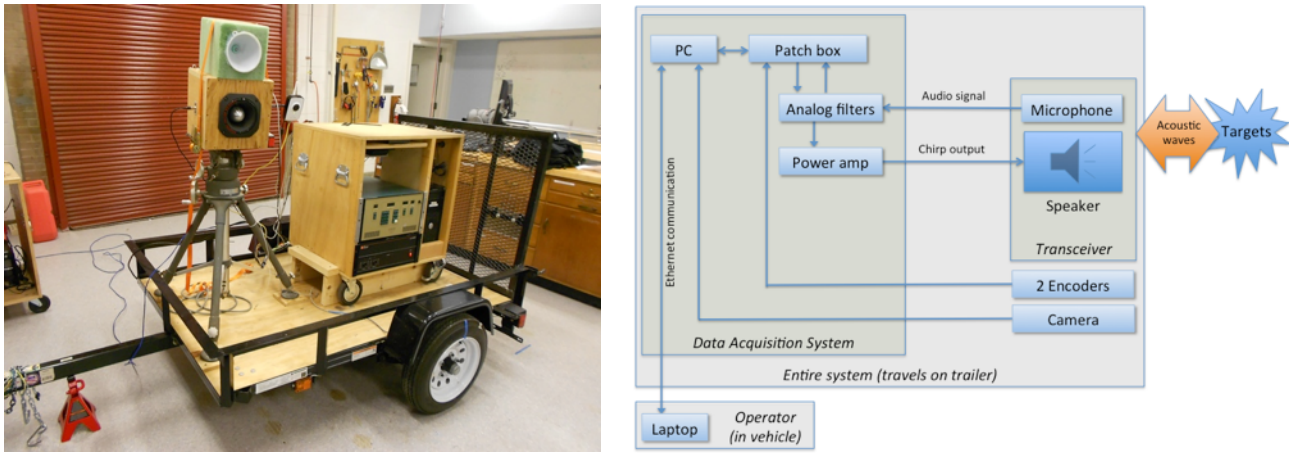

Figure 1: (left) Photograph of the SAA system. (right) Schematic of the system highlighting the various signal paths.

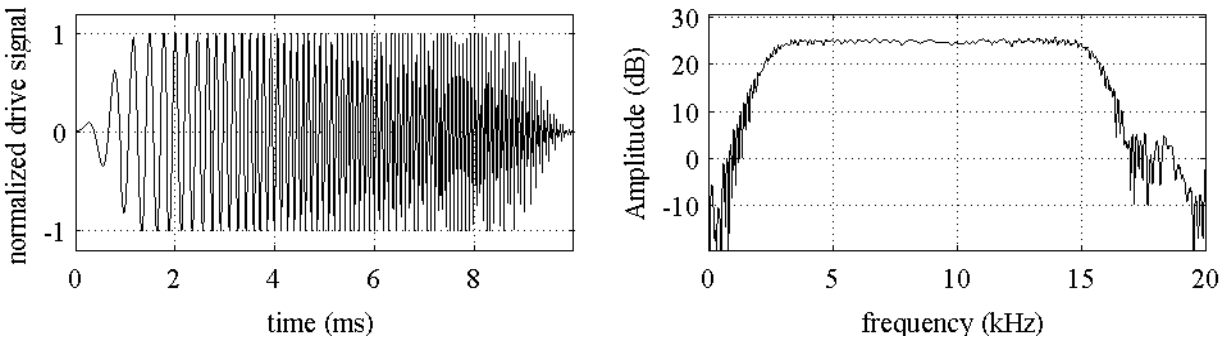

Figure 2: The 10ms excitation signal in time and frequency domain, indicating that the excitation frequency is flat from about 3 to 15 kHz.

The chirp, created on the data acquisition PC, is converted from digital to analog and delivered to the loudspeaker through the power amplifier. This excitation signal is broadcast repetitively at 40ms increments as the transceiver travels along the target path. The microphone simultaneously records the sound reflected from the scene. The signal is acquired at a sample rate of 80 kHz, and an antialiasing filter with a cutoff frequency of 25 kHz is used to condition the microphone signal. The sound pressure level delivered to objects in the target scene varies with range but is typically <105 dB, and the objects of interest are within 6 m of the transceiver. The transceiver assembly is angled at 18° below horizontal to improve imaging of the cords. The acquired audio signal is reshaped into a 2-D array such that each column contains 40 ms of data, beginning with the point corresponding to the beginning of each excitation broadcast. Since outdoor measurements can include significant wind-induced low frequency noise components, a high-pass filter is implemented to suppress such contamination below 1 kHz. A matched filter based on the source chirp is then used to range-compress the audio signal. The image is reconstructed by phase delaying individual received signals to correlate to each of the field locations[3].

3. PATH CORRECTION

In any realistic field application, the trailer path will not be straight. As a result, a path correction operation is used to compensate for path deviations. The encoders attached to the wheels of the trailer are sampled evenly in time and each

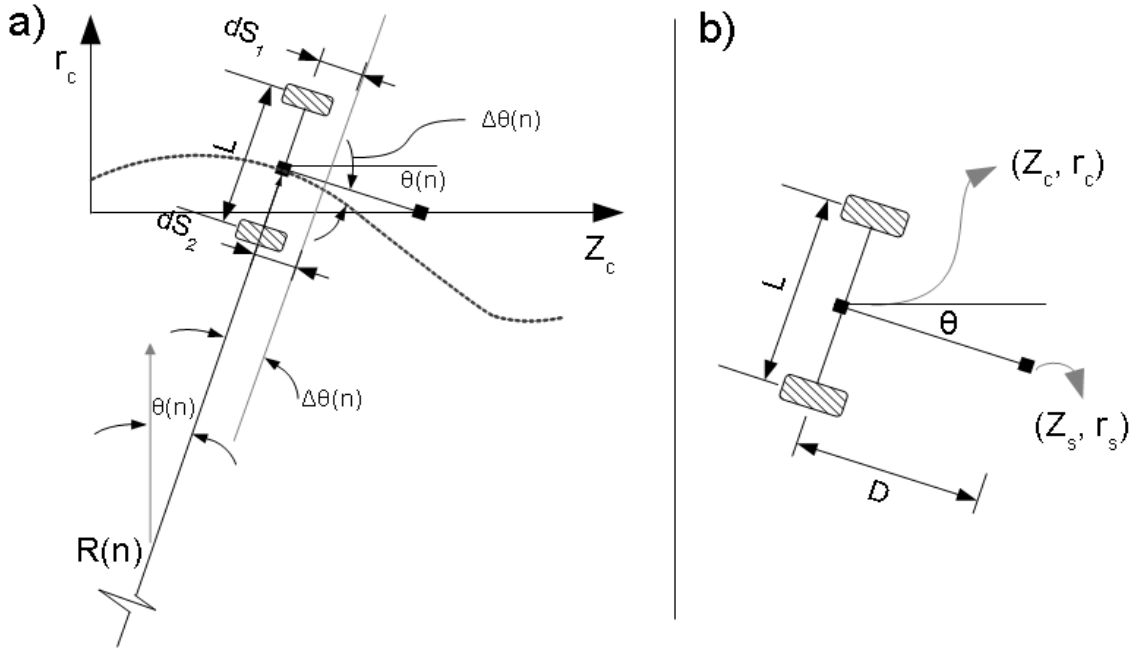

Figure 3: (a) Trailer path geometry. (b) Transceiver position (Z_s, r_s) related to the axle center position trailer (Z_c, r_c).

produces a sequence of positions once the tire circumference and gear ratio for the encoder wheel are considered. The geometry of the path of the trailer is shown in figure 3(a). In this figure, the z-axis is the nominal travel axis and the r-axis is the nominal direction of propagation of the outgoing sound.

The distance each wheel center travels during a sample interval is related to the travel geometry by the following equations:

$$ds_1(n) = \Delta\theta(n)\left(R(n) + \frac{L}{2}\right) \tag{1}$$

$$ds_2(n) = \Delta\theta(n)\left(R(n) - \frac{L}{2}\right) \tag{2}$$

where $\Delta\theta(n)$ is the change in the trajectory angle and $R(n)$ is the radius of curvature in the nth time interval. Solving for $R(n)$ from the equations above results in the following expression for the radius of curvature:

$$R(n) = \frac{L}{2}\left(\frac{ds_1(n) + ds_2(n)}{ds_1(n) - ds_2(n)}\right) \tag{3}$$

Subtracting eqn. (2) from eqn. (1) results in an equation for the change in trajectory angle.

$$\Delta\theta(n) = \frac{ds_1(n) - ds_2(n)}{L} \tag{4}$$

The equations for change in trajectory angle and radius of curvature can be rewritten as

$$R(n) = L\frac{d\bar{s}(n)}{\Delta ds(n)} \tag{5}$$

$$\Delta\theta(n) = \frac{\Delta ds(n)}{L} \tag{6}$$

where $d\bar{s}$ denotes the average of ds_1 and ds_2 , and $\Delta ds(n)$ represents the difference, $(ds_2 - ds_1)$. As illustrated in Fig. 3(b) z_c and r_c denote the position coordinates of the center of the trailer axle at the n^{th} moment in time. z_s and r_s denote the position coordinates of the transceiver. D represents the distance of the acoustic transceiver from the center of the axle. The path can be calculated by stipulating that both encoders and starting position all have an initial condition of zero and the travel direction is along the z-axis.

The following equations below along with the sampled encoder data can be used to calculate the instantaneous position of the trailer's axle center. The changes in the axle center coordinates are given by

$$\begin{aligned} \Delta z_c(n) &= d\bar{s}(n)\cos\left(\theta(n)\right) \\ \Delta r_c(n) &= d\bar{s}(n)\sin\left(\theta(n)\right) \end{aligned} \tag{7}$$

and

$$\begin{aligned} z_c(n+1) &= z_c(n) + \Delta z_c(n) \\ r_c(n+1) &= r_c(n) + \Delta r_c(n) \\ \theta_c(n+1) &= \theta_c(n) + \Delta\theta_c(n) \end{aligned} \tag{8}$$

The acoustic transceiver is a distance D in front of the trailer axle as shown in Fig. 3 and the instantaneous position is given by the following equations:

$$z_s(n) = z_c(n) + D\cos\left(\theta(n)\right)$$
$$r_s(n) = r_c(n) + D\sin\left(\theta(n)\right) \tag{9}$$

4. DATA ANALYSIS OF NON-METALLIC CORDS

The SAA system was used to study the detectability of a set of cords laid on an asphalt surface. The asphalt surface was nominally flat and clear of debris. Detection of non-metallic targets via acoustics is of interest because of the low radar scattering cross-section of such objects. Experiments were conducted on an empty parking lot on the campus at the Catholic University of America, with low levels of typical ambient urban noise, including pedestrian, wind, automobile, and air traffic background noise. Six braided nylon cords with diameters 3.2, 4.8, 6.4, 9.5 12.9 and 15.9 mm (1/8, 3/16, 1/4, 3/8, 1/2, and 5/8 inch) and a joined pair of fiber optic cables 3 mm in diameter were laid at 4 angles (0°, 10°, 20° and 30° from parallel to the travel path). Figure 4 shows the nylon cords and shielded fiber optic cable used as targets to be imaged. The imaged scenes also include paved ground surfaces, and metal retro-reflectors added to the image as fiducial markers. Figure 4 also shows the location at which the data was collected.

For each data collection, the SAA system trailer was towed behind a pickup truck at speeds between 0.5 and 1 mph. Future improvements to the system, including broadcasting of diverse pulses at a faster repetition rate, will allow for increased vehicle speed. There is essentially no limit to the duration for which data can be collected (other than that imposed by the finite storage space for data on the PC's drive), and for the results presented here, that the total distance traveled is typically over 65 m. The resolution of the image is therefore not limited by the aperture created by the sensor

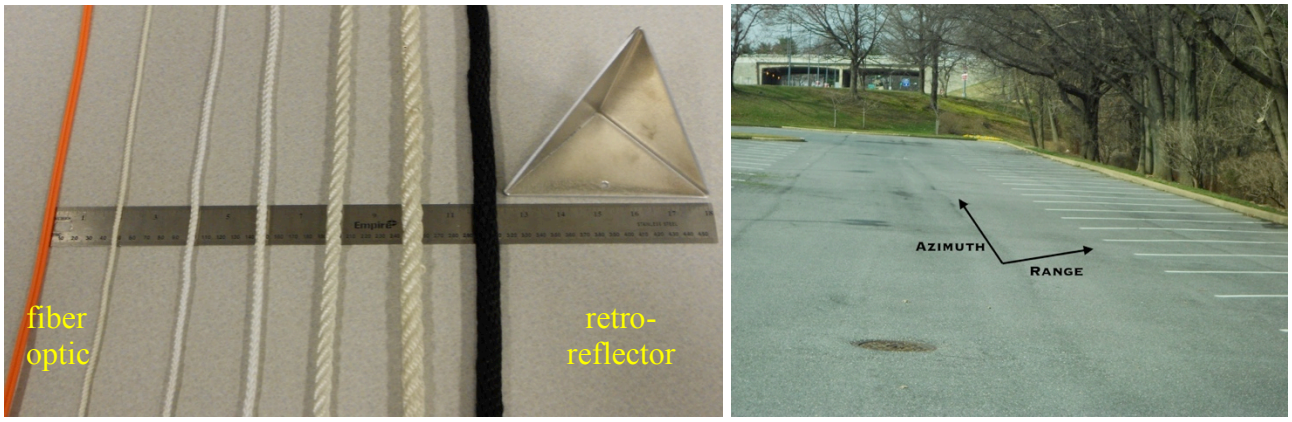

Figure 4: (left) Photograph of fiber optic cable, braided nylon ropes of various diameters, and metal retro-reflector used as a fiducial marker. (right) Photograph of data collection scene (without targets).

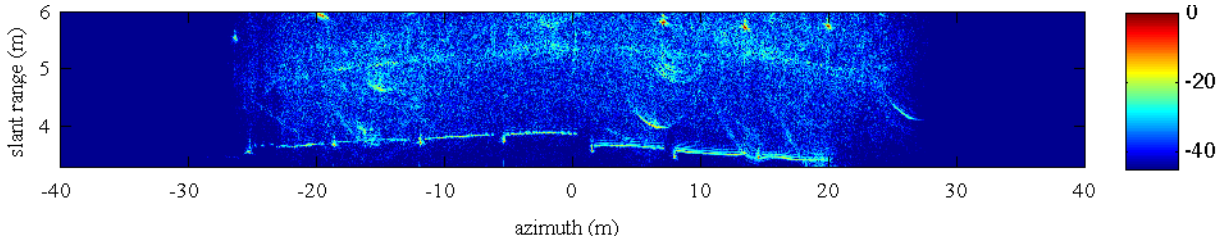

Figure 5: Reconstructed, path-corrected image of seven cords positioned nominally parallel to transceiver path at a slant range of 3.7m. Diameter of nylon cords decrease from right to left. The fiber optic cable is the cord in the set on the left side. Other scatterers in the measurement field include a long seem in the asphalt that extends over the full azimuth of the image at a nominal slant range of 5m as well has other faults in the pavement and retro-reflector fiducials placed in know lactations to cords.

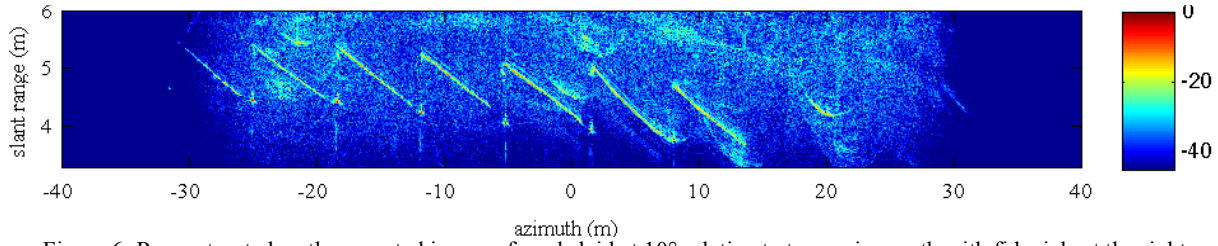

Figure 6: Reconstructed, path-corrected image of cords laid at 10° relative to transceiver path with fiducials at the right end of each cord and less than 0.5 m below the left end of each rope.

motion, but by factors such as directionality of the speaker and microphone and the decrease in sound pressure level due to spherical spreading with range.

Figure 5 shows the path corrected reconstructed image of the data collection with the cords parallel to the trailer direction of travel (azimuth). For this data collection set the image is displayed with a 60m azimuth and a range of 3 - 6m. All of the cords are clearly visible in the image. The six nylon cords decrease in diameter from right to left, with the 7th cord being the fiber optic cable. For all data collection sets the cords were kept in that order. The fiducial markers are also visible at the left end of each cord and at the top of the image. Note that the cords are not perfectly aligned with each other as can be clearly seen from the reconstructed image.

The reconstructed image of Fig. 6 show all cords laid out at 10° to trailer direction of travel with an azimuth of 60 m and range of 3.5 – 6 m. Note that the vertical and horizontal scales in the plots differ, causing the 10° angle of the cords to appear exaggerated. The fiducial markers can be seen to the right of each cord and at the top of the image. Again all cords are clearly visible. In addition, to the right of the first cord (largest diameter, rightmost in Fig. 6), at approximately 4.3 m and an azimuth of +20 m, is the image of a small tree branch unintentionally left in the collection scene.

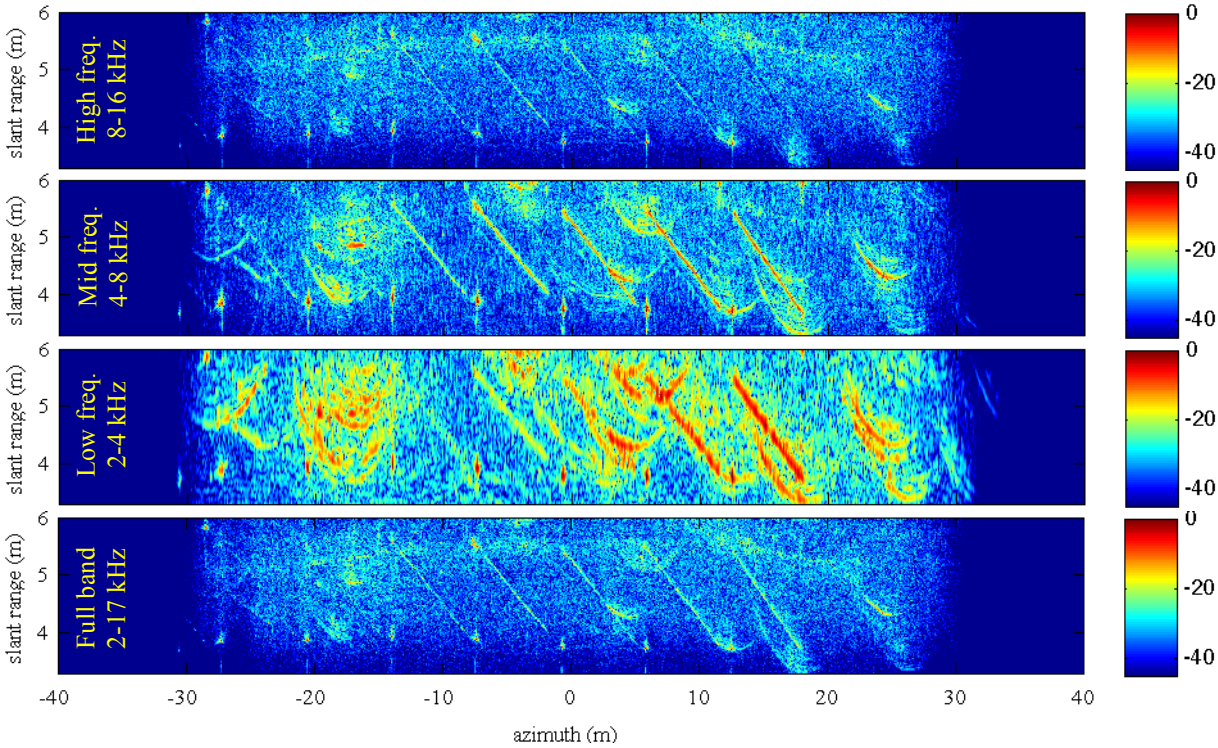

Figure 7: Reconstructed, path-corrected images of cords at 20° relative to transceiver path. *Bottom*: Full frequency band, 2-17 kHz, *Second from bottom*: Low frequencies, 2-4 kHz, *Second from top*: Middle frequencies, 4-8 kHz, *Top:* High frequencies, 8-16 kHz.

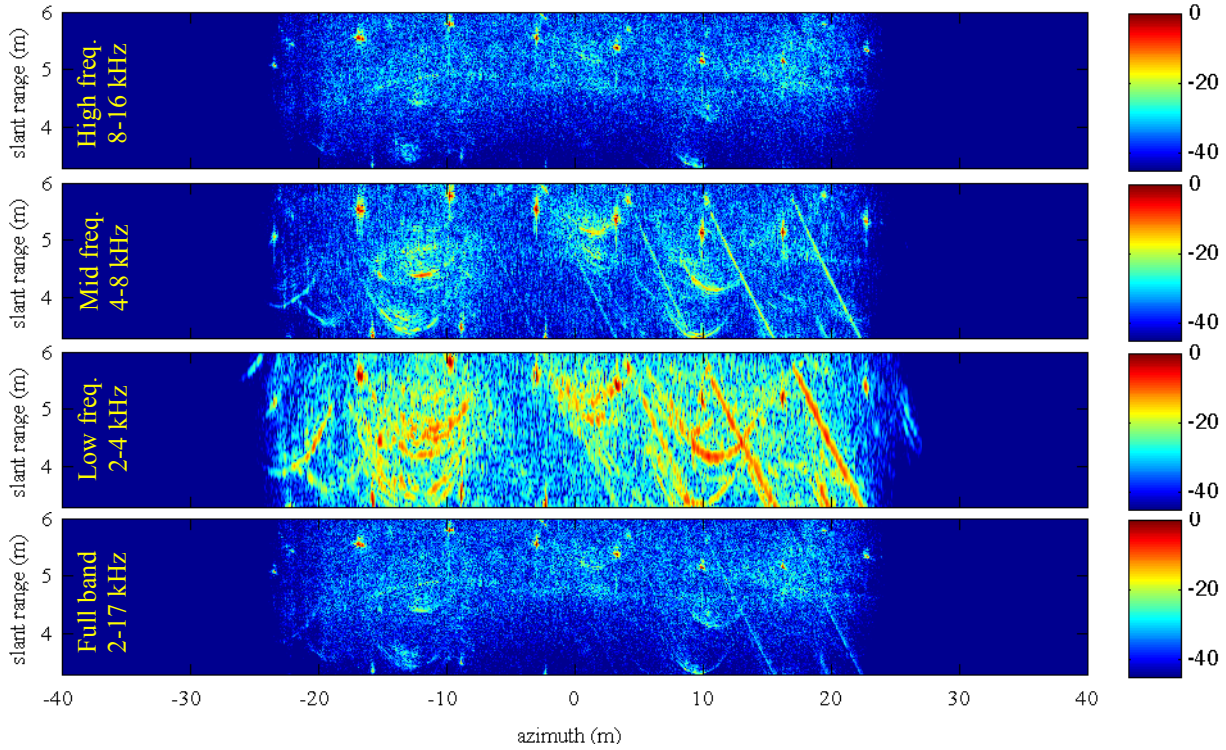

Figure 8: Reconstructed, path-corrected images of cords at 30° relative to transceiver path. *Bottom*: Full frequency band, 2-17 kHz, *Second from bottom*: Low frequencies, 2-4 kHz, *Second from top*: Middle frequencies, 4-8 kHz, *Top:* High frequencies, 8-16 kHz.

As the angle of the ropes relative to the trailer's direction of travel is increased to 20° as shown in Fig. 7 (*bottom*), the visibility of 6th and 7th cord (smallest diameter nylon cord and fiber optic cable) is completely lost. Of the remaining cords though still visible, their acoustic return is not as strong as the 0° and 10° data set. In further analysis, the frequency content is separated into three octave bands of 2–4 kHz, 4–8 kHz and 8–16 kHz. In the low band, Fig. 7 (*3rd from top*), the larger diameter cords (15.9 – 9.5mm) cords can be seen clearly with high signal-to-noise ratio. At mid-band Fig.7 (*2nd from top*), only five of the seven cords (decreasing diameter) are clearly visible, along with the fiducial markers. However, in the mid-frequency band the image of the cords are more distinct than any other bands except for the larger diameter cords in the low frequency (2-4kHz) band. In the 8-16 kHz band, Fig. 7 (*top*), the 4.8mm, 6.4mm and 9.5mm diameter nylon cords can be seen but as very weak return images with the rest of the cords barely noticeable.

The images of Fig. 8 (*bottom*) show the cords at 30° to the trailer direction of travel. In this 30° configuration only two of the large diameter (12.9 and 15.9 mm) cords are visible along with a few of the fiducial markers. The frequency content of this data set is also separated into the three octave bands described previously. Again, the low band, Fig. 8 (*3rd from top*), amplifies the image of the large diameter cords and all information about the smaller diameter cords is lost. The mid-band Fig. 8 (2nd *from top*) also shows the large diameter cords and fiducial markers, along with the image of two additional smaller diameter cords that were not visible in the wide band (2-17 kHz). Finally, the high-band Fig. 8 (*top*), only shows the image of the fiducial markers are visible and all imagery of the cords is lost.

5. CONCLUSIONS

This work has been conducted to demonstrate the ability of side-scanning synthetic aperture using acoustic radiation to detect non-metallic cords, which cannot be detected by its counterpart, SAR. Analysis of the collected data has shown that the detectability of the cords in the presence of ambient noise depends on parameters such as cord angle relative to the transceiver path, characteristics of the excitation signal including chirp repetition rate and duration, source signal

amplitude and directionality of transceiver. The results also show that detection of the cords is sensitive to the angle relative to the transceiver path, with strong detection at small angles. The additional images produced from dividing the frequency band into these octave bands for the 20° and 30° data set show that this can enhance detectability, qualitatively speaking. For this specific case, the results showed the optimum band of detection to be the 4-8 kHz.

Detection using the SAA system has shown valuable promise with the ability to detect centimeter scale non-metallic targets. The system is cheaper than SAR, relatively easier to build and can be a complement to a radar system greatly enhancing the overall detection ability. With subsequent signal processing algorithms, the system will be taken to the next level in which material properties of targets may be inferred from the collected data.

6. ACKNOWLEDGEMENTS

This work was conducted as part of a grant from the Army Research Office and supported by the US Army RDECOM CERDEC Night Vision and Electronic Sensors Directorate.

REFERENCES

[1] S. Bishop*, et al.*, "Outdoor synthetic aperture acoustic ground target measurements," presented at the SPIE Defense Sensing, 2010.
[2] Raney, R. K., 1971, “Synthetic aperture imaging radar and moving targets,” *IEEE Transactions on Aerospace and Electronic Systems*, AES-7, pp. 499-505.
[3] Vignola, J. F., Judge, J. A., Good, C. E., Bishop, S. S., Gugino, P. M., and Soumekh, M., 2012, “Detection of non-metallic cords using synthetic aperture acoustic imaging,’ *Sensing and Imaging*, in press. Wehner, D. R., 1987, *High Resolution Radar*, Artech House, Inc., Norwood, MA.
[4] Wehner, D. R., 1987, *High Resolution Radar*, Artech House, Inc., Norwood, MA.
[5] Soumekh, M., 1999, *Synthetic Aperture Radar Signal Procession*, Wiley-Interscience.